

Comparing and Enhancing the Analytical Model for Exposure of a Retail Facility Layout with Human Performance

Abstract ID: 1266

Bradley Guthrie, Pratik J. Parikh, Tyler Whitlock, Madison Glines, Thomas Wischgoll, John Flach, and Scott Watamaniuk
Wright State University
Dayton, OH 45435 USA

Abstract

Recent research in retail facility layout has focused on developing analytical models to *estimate* visibility measures of novel rack layouts based on assumptions about a shopper's field of view. However, because of the human element involved in the shopping experience, it is vital to compare these models relative to actual human performance. In this study, we evaluate the predictions of our previously developed analytical model (that estimates exposure of every location on a given rack layout assuming expected head movement) in a 3D Virtual Environment (VE). We conducted trials with 18 participants who were asked to find targets strategically placed on the racks for 9 unique layouts. A comparison of their performance with the analytical model suggested that our model performed well, but the performance varied across layouts. To enhance these exposure estimates from the analytical model, we combined it with parameters corresponding to human head movement collected from the VE study, along with layout and target location parameters, in a decision tree framework. Results indicate that combining analytical and empirical observations enhances the quality of estimates (test AUC = 0.9).

Keywords

Retail layout; exposure; human subjects; virtual environment

1. Retail Facility Layout

The facility layout in a retail setting plays an important role in the presentation of products to customers [1]. In fact, sales are a function of the number of people who are exposed (visually connected) to products [2]. As such, researchers have widely alluded to product exposure as a measure of importance for retail layout design [3]. Designing retail layouts catered to human visibility would potentially result in reduced search time for already planned purchases, as well as influence shoppers to make more unplanned purchases. Retail managers meanwhile would benefit by strategically placing their products in 'hot spots' potentially increasing impulse purchases.

Our motivation for evaluating layouts based on exposure primarily stems from our personal visits to local retail stores, as well as discovery of up-and-coming retail layouts online (Figures 1-3). Racks placed at a more acute orientation could provide better alignment with human vision. Curved racks potentially allow shoppers to have a better view of products deep in the aisle, and can be visually more appealing. Many studies in the retail domain address or allude to human visibility, from both analytical [4,5] and empirical perspectives [6]. However, these studies do not

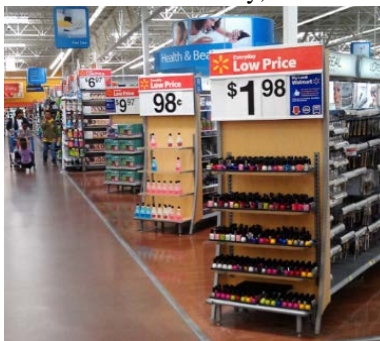


Figure 1. Racks oriented at 45°

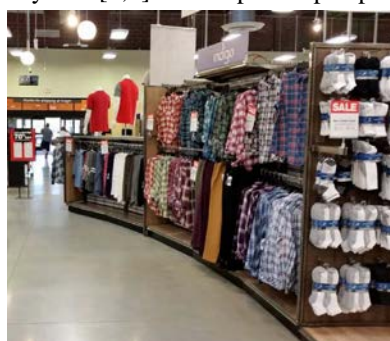


Figure 2. Curved racks



Figure 3. Curved endcaps

consider the effect of layout (e.g., rack orientation and curvature) on shopper visibility. The existing analytical approaches also lack comparisons of their models to human behavioral data.

The objective of this research is to compare our previously proposed analytical models with human performance through a study in a virtual store. That is, if our models suggested that orienting racks differently from a standard 90° would aid shoppers visually connect with more products, do actual shoppers experience that? What if the racks were curved as in Figure 2? Further, how would varying orientation and curvature affect the scanning pattern of shoppers? Would different layouts influence shoppers to make larger head rotations, or even increase the speed of their scanning? Using this information, we not only *compare* the performance of our analytical models with human performance, but also *enhance* the model’s predictions with key human performance factors to increase the quality of prediction. The main goal is to use such a combined analytical-empirical model in optimizing the rack orientation and curvature to meet specific objectives; e.g., maximizing impulse purchases due to increased product exposure (for the retailer) and/or minimizing search time (for the shopper).

2. Existing Analytical Exposure Models with Human Vision

Mowrey et al. [7] recently proposed an analytical model and an algorithm to capture the dynamic interaction between a walking shopper’s 2D field of regard (FoR) – the angular size of possible viewing angles for a fixation point – and a static layout of racks. They evaluated both exposure and intensity (time of exposure) of racks for varying orientations (θ).

Guthrie and Parikh [8] expand their work to model this interaction in 3D, while also considering both the curvature (α) and height of racks. Figure 4 illustrates how they model a shopper 3D FoR. They consider angular limits of vision in both horizontal and vertical dimensions (Figures 4(a) and (d)), along with the depth of vision (DOV). The combination of both horizontal and vertical limits is modeled as an elliptical sector of a sphere; see Figure 4(c), where they further break down these limits by head (Ω) and eye (Φ) rotations.

To illustrate how this shopper FoR interacts with a layout of racks, Figure 5 contains two layouts (θ =orientation and α =curvature) with overlaid profiles of the intensity of exposure (red = longest exposed, yellow = shortest exposed, white = not exposed). Notice the different intensity levels starting from rack 2 between these figures, which occur due to the dynamic interaction of the shopper FoR with the curvature and orientation of the racks, and the resulting obstruction of the shopper FoR.

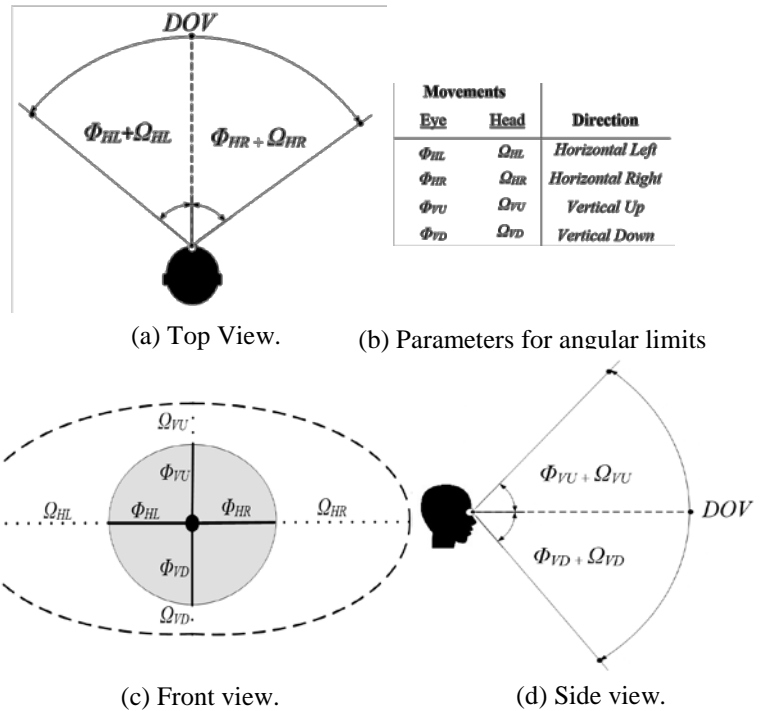
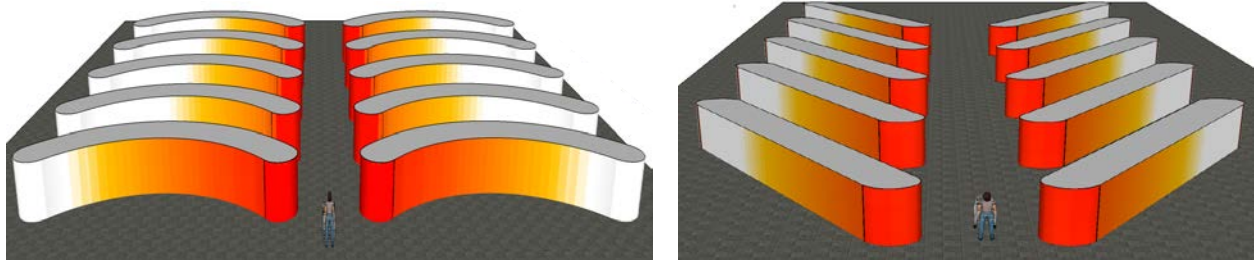


Figure 4. Modeling a 3D FoR.



(a) Intensity of exposure for $\theta=90^\circ$ and $\alpha=90^\circ$

(b) Intensity of exposure for $\theta=30^\circ$ and $\alpha=0^\circ$

Figure 5. Rack layout with overlaid intensity

3. Virtual Environment for Comparing the Analytical Model with Human Performance

For this comparison, we evaluated human performance in a virtual environment (VE). This study was approved by Wright State University’s Institutional Review Board (IRB).

3.1 VE Setup: The VE utilizes 27 LCD screens with LED backlight (each 55” in size) to create a three-walled CAVE-type immersive display to a height of 87 inches surrounding a 12x12 sq. ft. walkable area (see Figure 6). The optical tracking system composed of 11 cameras provided maximum redundancy and accuracy to track the user’s head position. Based on that head position, the system recreates the user’s perspective view on all 27 displays in such a way that the user feels completely immersed in the scenario. A head tracker captures both horizontal (x-axis) and vertical (z-axis) head movements made by the human participant. Additional details about the VE setup can be found in Wischgoll et al. [9].



Figure 6. The VE set up; our co-author pictured

3.2 Study Design: We recruited 18 participants (of which 9 were female) between the ages of 19-26 years (avg=21.4) who had several years of prior shopping experience, and all were right-handed. Eleven participants had corrected vision and wore their glasses; all passed a visual acuity test. Each participant was informed through an IRB consent process before participating. We limited our study to evaluating 9 rack layouts comprising all combinations of 3 values each of theta and alpha ($\theta = 45^\circ, 90^\circ, 135^\circ$ and $\alpha = 0^\circ, 30^\circ, 90^\circ$). All racks were above the participant’s eye height. Participants evaluated all 9 layouts over a 1-hour study period (including training). For each layout (containing 10 racks on either side), a participant was asked to search for targets (12 red colored squares, 1”x1” in size) strategically placed on the front and back faces of the racks at distinct rows (i.e., heights) and columns (i.e., distance from walking aisle). The shopper’s walking along the aisle was simulated by configuring the VE to move at a speed of 3.33 fps (similar to 3.41 fps in Daamen [10]) while the participant remained stationary. We simulated bidirectional travel by first letting the racks pass by the shopper in one direction and then reversing the environment to let the racks pass by in the reverse direction for the same layout. Participants were asked to push a button on a wireless device and call out the aisle number and side (left or right) when they saw a target. We conducted a total of 324 trials (18 trials x 18 participants) while recording their head movements.

4. Observed Human Behavior and Performance in the VE

Since we were able to record the actual head movements for each participant, we derived several measures to broadly analyze their scanning patterns. For this study, we focus on horizontal scanning patterns; vertical scans were relatively consistent with minimal variance and thus are not discussed. First, we calculated both the ‘average head rotation’ and the ‘maximum head rotation’ specific to each layout (in both forward and reverse directions). Figure 7 shows the time history for angular position (horizontal) for one participant in a layout with $\theta=135^\circ$ and $\alpha=0^\circ$.

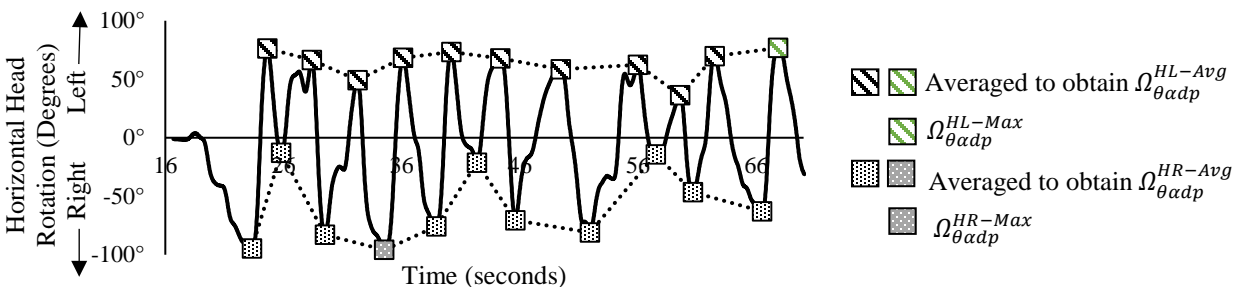


Figure 7. Head Rotation (horizontal) for single participant run

Each time the participant’s head rotated across the center line of their pathway (0°), we recorded the maximum angle of the head turn. To derive an ‘average head rotation’ for each participant (p), we subsequently averaged these values (left and right, separately) across all orientations (θ), curvatures (α), and directions (d); these are notated as $\Omega_{\theta\alpha d}^{HL-Avg}$ and $\Omega_{\theta\alpha d}^{HR-Avg}$, respectively. Averaging across both directions and across all participants helps estimate the overall ‘average head rotation,’ $\Omega_{\theta\alpha d}^{H-Avg}$. Similarly, we derive the average ‘maximum head rotation’ across the two sides and all participants as $\Omega_{\theta\alpha d}^{H-Max}$.

Further, we derived the average angular speed (degrees/second or deg/s), average crossing speed (deg/s), number of center crosses, bias, and extreme head activity. Average angular speed was calculated by taking the average change in head position (over an increment of 0.001 sec) divided by the total run time. The number of center crosses was calculated as the number of times participants’ heads rotated across the center point of the display (i.e., 0° line in Figure 7). Crossing speed is the average instantaneous velocity of a participant’s head rotation for all crosses in a run. Bias was defined as the proportion of time a participant’s head position was left of the center line, whereas ‘absolute bias’ represents the magnitude to which a participant favored either the right or left side. This is estimated as $|0.5 - \text{bias}|$. We define extreme head activity as the proportion of time where speed of head position was above 100 deg/s or acceleration above 500 deg/s². This can be a factor in a participant not seeing a target due to such fast head movement.

Figure 8 depicts the normalized averages across 18 participants for each measure visualized as a star plot, for all 9 layouts. Values are normalized linearly on a 0-1 scale for each measure; 1 corresponds to the outer gridline, 0 is the center. Observing in Figure 8(a) the relatively high values of average angular speed, average head rotation, maximum head rotation, and extreme head activity for θ values of 135°, followed closely by 90°; these measures are close to 0 for $\theta = 45^\circ$. This is because rack orientations of 90° or greater required the shopper to use faster and larger head rotations to closely align their head rotation angle to the orientation of the racks given the constant forward translation. For racks oriented at 45°, however, much less head movement was required to see both rack faces.

Further, racks oriented at 90° resulted in participants being more biased toward one side versus the other, in addition to making a minimal number of crosses at relatively high speeds. These movements may be due to the relatively condensed space for these layouts (i.e., deviations of θ and α from 90° and 0° result in increased floor space and travel path – space models not included due to space limitations), exposing participants to view a relatively large quantity of rack area per unit of time along their path. For reverse travel in each of these layouts, similar, but opposite patterns were observed likely because the angles in the reverse direction are complementary to the forward travel. So for the same participant, the behavior for $\theta = 135^\circ$ in the forward direction would closely resemble that for $\theta = 45^\circ$ in the reverse direction (Figure 8(b)).

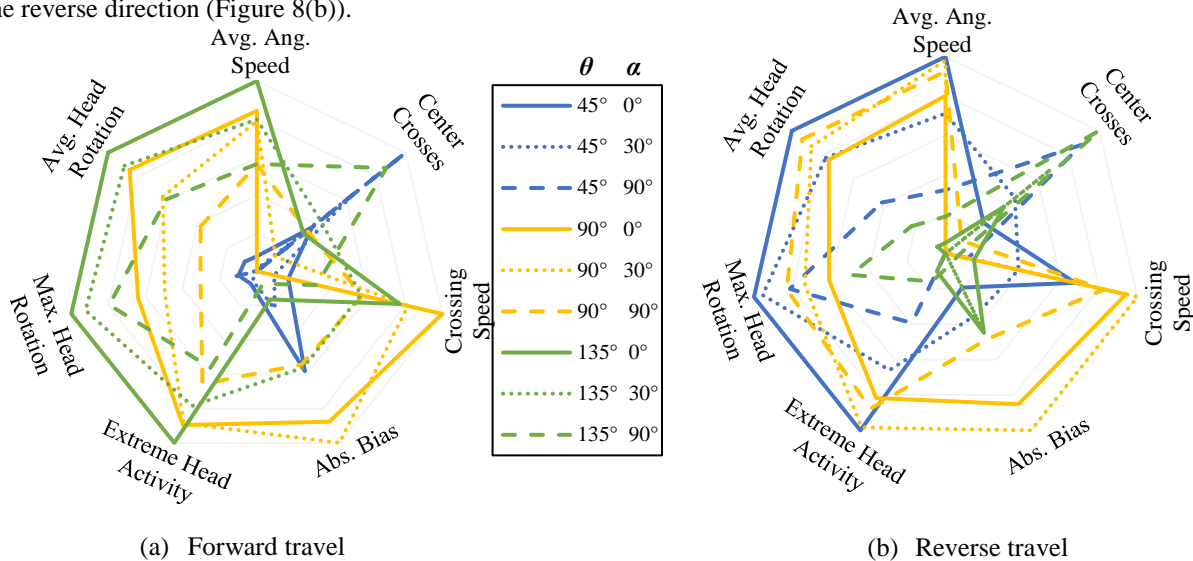


Figure 8. Normalized scanning pattern measures averaged across 18 participants

5. Comparison of the Exposure Models with Human Performance

We compare predictions from our analytical model (where estimated intensity ≥ 1 s meant shopper is exposed to the target) with human performance data. Based on whether a participant sees a target (i.e., a ‘hit’) or does not see it (i.e., a ‘miss’), targets are classified as either *true positive* (TP or predicted hits; i.e., model predicts participant will see and participant actually sees), *false positive* (FP or unpredicted hits; i.e., model predicts participant will see, but participant does not see), *true negative* (TN or predicted misses; i.e., model predicts participant will not see and participant does not see) and *false negative* (FN or unpredicted misses; i.e., model predicts participant will not see, but participant sees). To then assess the performance of our model, we calculated the positive prediction value (PPV), negative prediction value (NPV) and accuracy (ACC), where $PPV = \frac{TP}{TP+FP}$, $NPV = \frac{TN}{TN+FN}$, and $ACC = \frac{TN+TP}{TN+FN+TP+FP}$. The PPV measure fundamentally tells us, ‘for targets our model predicted to be *seen*, what proportion were actually *seen*?’ NPV contrarily answers ‘for targets our model *did not* predict to been seen, what proportion were actually *not seen*?’ The ACC measure however represents $(1 - \text{total error rate})$, where the error rate accounts for both overestimates (FN) and

underestimates (FP). Figure 9 contains average values (across all participants for each layout); global averages were $PPV=0.82$, $NPV=0.72$, and $ACC=0.77$. Layouts with $NPV=0$ contained no targets not predicted to be seen.

These results indicate that our analytical exposure models performed fairly well on certain layouts. For instance, for layouts with $\theta=135^\circ$, (forward travel) and $\theta=45^\circ$ (reverse travel), the PPV was 1.0 and 0.98, respectively; ACC was acceptable too, 0.85 and 0.80, respectively. On the contrary, our models performed relatively weaker for layouts with $\theta=45^\circ$, (forward travel) and $\theta=90^\circ$ (reverse travel); $PPV=0.71$ and 0.81 ($ACC=0.70$ and 0.71), respectively. One possible explanation for these differences may be the distribution of intensity values for specific layouts. For instance, the average intensity value of targets predicted to be seen for layouts with $\theta=135^\circ$, (forward travel) and $\theta=45^\circ$ (reverse travel) were 6.7 and 6.8 seconds respectively, whereas those for layouts with $\theta=45^\circ$, (forward travel) and $\theta=90^\circ$ (reverse travel) were 3.9 and 4.2 seconds respectively. Participants were more likely to see targets with higher intensity values in the former instances, leading to a higher match with the predictions from the analytical model; recall, if the intensity is >1 second, the analytical model would mark it as likely seen.

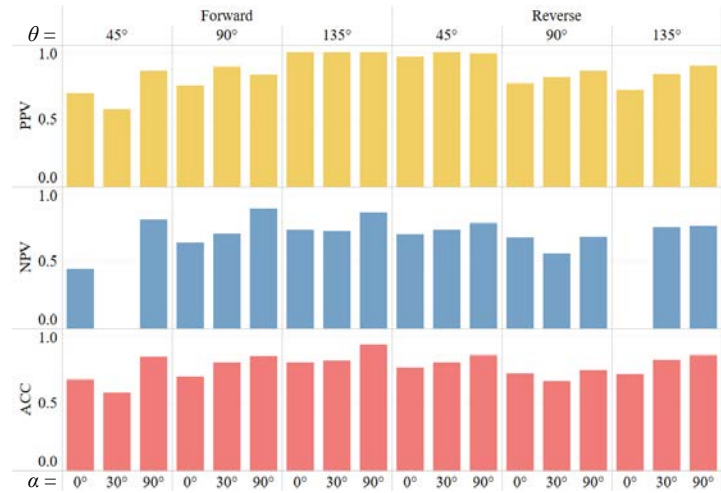


Figure 9. PPV, NPV, and ACC averaged across 18 participants

6. Enhancing the Analytical Exposure Models with Human Behavior

Considering that the participants altered their scanning pattern based on the layout (whereas our analytical model assumed a single, fixed, FoR for all layouts), we sought to utilize these unique scanning patterns to enhance the quality of exposure predictions from the analytical models. As a first step, we combined both the analytical estimates and human behavior measures into a prediction model using decision trees. We chose this non-parametric approach for two reasons; first, the normality and relevant assumptions for use of ANOVA could not be verified, and second, the decision tree model aids in intuitive analysis via if-then rules. We built four decision tree models, each with an incremental addition of factors. Model 1 uses only the analytical model (AM) estimates (i.e., estimated intensity of exposure of a target in seconds). Model 2 included layout and target parameters (e.g., θ , α , direction, target location quantified as the row and column on a rack). Models 3 and 4 included human behavior factors (from Section 5); Model 3 was allowed limited number of splits, while Model 4 was allowed to have unlimited splits. We used a train-validation-test approach (60:20:20 split of 324 data elements), where the validation data was used to stop model training to avoid overfitting.

Table 1 summarizes the performance of these models on AUC (area under the ROC curve) and test ACC. Notice that the Test AUC (measure of the model's performance on unseen data), is reasonably high just with the predictions from the AM (Model 1). The other models show the incremental benefits to the Test AUC.

Table 1. The four enhanced exposure models based on decision trees

#	Factors included in the Decision Trees	# of Splits	AUC			ACC
			Train (60%)	Validation (20%)	Test (20%)	Test (20%)
1	Analytical Model (AM)	21	0.861	0.857	0.860	0.795
2	AM + layout + target	29	0.923	0.905	0.890	0.818
3	AM + layout + target + human (limited splits)	27	0.922	0.881	0.889	0.828
4	AM + layout + target + human	63	0.938	0.908	0.912	0.835

Individual contributions of parameters for each model are shown in Table 2. The number of splits refers to the number of times a node is divided. G^2 is the likelihood ratio chi-square statistic (i.e., higher values indicate higher variation within a parameter with respect to the response). A deeper analysis of these decisions trees revealed that the root node (first split) in all the 4 models was always based on the intensity estimate from the AM. This is intuitive as the quality of prediction of the AM is already fairly high. After this, the next few splits were largely dependent on the location of the target (rack face, and target column) and the layout (orientation and curvature). Further, with the exception of average head rotation, the splits for human parameters in Models 3 and 4 were generally located towards the bottom of the decision trees (farthest from the root node). In both models, average head rotation occurred as the 2nd split for lower intensity values. In other words, if intensity values were low, the odds of a participant seeing the

target were highly dependent on the average extent to which they rotated their head. Overall, Models 2 and 3 appear to strike a good trade-off between the quality of exposure predictions for a layout and the model's complexity.

7. Conclusion and Next Steps

The objective of this study was to compare the findings from a recently proposed analytical model (for estimating exposure of racks in a 3D retail store) to human performance. To do this, we designed a virtual environment of a retail rack layout, where curved racks were placed at various orientations. We asked 18 participants to search for targets in 9 unique layouts. Our trials revealed substantial variation in the head movement of these participants. The analytical model, that assumed an expected horizontal head movement with a single scan at each shopper step, appeared to perform reasonably well. However, further enhancements to the exposure estimates are possible with the inclusion of target and layout parameters in a decision tree framework. The inclusion of human behavior parameters further increased the prediction quality, but only marginally. Essentially, both Models 2 and 3 seem to provide good tradeoff in terms of quality of estimates and complexity.

As next steps, we plan to use either Model 2 or 3 as exposure estimates in an optimization model to determine the optimal rack orientation and curvature that maximizes total exposure under space constraints. If possible, we will derive expected impulse purchase (retailer) and improved experience (shopper) as functions of total exposure of a layout in subsequent optimization models.

Acknowledgements

This research was partially supported by the National Science Foundation grant CMMI #1548394.

References

1. Dunne, P. M., Lusch, R. F., and Gable, M. (1995). *Retailing*. Cincinnati, OH: South-Western College Pub.
2. Cairns, J. P. (1962). Suppliers, retailers, and shelf space. *Journal of Marketing*, 34-36.
3. Sorensen, H. (2009). *Inside the mind of the shopper: The science of retailing*. FT Press, NJ.
4. Peters, B. A., Klutke, G.-A., and Botsali, A. R. (2004). Research issues in retail facility layout design. In R. D. Meller, M. K. Ogle, B. A. Peters, G. D. Taylor and J. S. Usher (Eds.), *Progress in Material Handling Research: 2004* (pp. 399-414).
5. Yapicioglu, H., and Smith, A. E. (2012). Retail space design considering revenue and adjacencies using a racetrack aisle network. *IIE Transactions*, 44(6), 446-458.
6. Phillips, H. (1993). How customers actually shop: Customer interaction with the point of sale. *Journal of the Market Research Society*, 35(1), 51-63.
7. Mowrey, C. H., Parikh, P. J., and Gue, K. R. (2017). The impact of rack layout on visual experience in a retail store. *INFOR: Information Systems and Operational Research*, 1-24.
8. Guthrie, B. and Parikh, P. J. (2017). Analyzing a shopper's visual experience in a retail store in 3D. In *IISE Annual Conference. Proceedings* (pp. 746-751), Pittsburgh, PA.
9. Wischgoll, T., Glines, M., Whitlock, T., Guthrie, B., Mowrey, C., Parikh, P. J., and Flach, J. (2017), *Display infrastructure for virtual environments (DIVE)*, in press, *Journal of Imaging Science and Technology*.
10. Daamen, W. (2004). *Modelling passenger flows in public transport facilities* (doctoral dissertation). Netherlands Research School for Transport, Infrastructure.

Table 2: Parameter contributions

Parameter	Splits	G ²	Parameter	Splits	G ²
<i>Model 1: Intensity</i>			<i>Model 4: All parameters</i>		
AM-Intensity	21	1167.5	AM-Intensity	10	1139.2
<i>Model 2: Intensity + layout + target</i>			Face (front/back)	6	168.9
AM-Intensity	7	977.5	Target column	6	147.3
Face (front/back)	4	222.7	Orientation	9	134.3
Target column	7	201.8	Avg. head rotation	5	109.7
Curvature	5	88.0	Curvature	6	90.2
Orientation	4	76.3	Avg. angular speed	4	63.2
Direction	1	25.2	Abs. bias	3	34.9
Target row	1	23.1	Direction	4	30.3
<i>Model 3: Intensity + layout + target + some human parameters</i>			Avg. crossing speed	3	29.9
AM-Intensity	5	968.6	Center crosses	2	26.1
Face (front/back)	4	186.0	Saccade time	2	25.9
Target column	7	163.4	Max head rotation	2	25.0
Curvature	5	92.9	Target row	1	7.7
Orientation	3	66.7			
Avg. head rotation	1	51.4			
Avg. angular speed	1	51.1			
Direction	1	18.1			